Adsorption of Atmospheric Gases at the Air−Water Interface. I. NH_3

D. J. Donaldson

Department of Chemistry and Scarborough College, University of Toronto, 80 Saint George Street, Toronto, Ontario, Canada M5S 1A1

Received: August 7, 1998; In Final Form: October 29, 1998

Several water-soluble vapors of atmospheric importance adsorb at the air−water interface. This paper supplies a thermodynamic and kinetic framework for analyzing this phenomenon. As an example, temperature- and time-dependent surface-tension measurements of aqueous ammonia solutions are used to extract the interfacial binding energies and evaporation rates. The standard Gibb's energy of adsorption of vapor-phase ammonia to the water surface is $-(19.1 \pm 0.5)$ kJ mol^{-1} at 298 K; the saturated coverage is $(1.2 \pm 0.2) \times 10^{14}$ molecules cm^{-2}. The Gibb's energy of activation for ammonia evaporation from the water surface lies in the range 13−18 kJ mol^{-1} at 298 K. Ab initio calculations of the NH_3-H_2O and $NH_3-(H_2O)_2$ complexes have also been performed to further understand the nature of the surface-bound species. The experimental and ab initio results, taken together, suggest that ammonia is bound by a small number (two or three) of water molecules at the surface; this complex species represents a "critical cluster" which is easily transferred into the bulk solution.

A. Introduction

The transport of trace gases across the air−water interface plays a crucial role in atmospheric chemistry. Many important chemical processes take place in the aqueous phase in the atmosphere, within or upon droplets of water or acids.[1,2] Therefore, understanding the specific interactions experienced by trace species at the air−water interface is of some importance. Recent work from this laboratory[3] and elsewhere[4,5] has shown that, for some species, a surface-bound or adsorbed state may be formed at this interface.

There are only a few studies in the literature of gas adsorption onto water surfaces.[3−14] Much of this has described the adsorption behavior of vapors of organic liquids onto water. Water acts as a substrate with a low surface energy compared to most solid surfaces but higher than most organic liquids. Therefore, vapors of hydrocarbon liquids, small chlorinated hydrocarbons, ethers, acids, and ketones adsorb to the water−air surface with standard enthalpies of adsorption similar to their $\Delta H°$'s of vaporization. Even relatively insoluble species, such as CCl_4 and benzene, exhibit this behavior, more commonly associated with heavy, long-chain amphiphiles.

The idea that soluble gases could adsorb onto a water−air interface, reducing the surface tension, was advanced in 1928 by O. K. Rice,[7] who measured the surface tension, σ, vs concentration for solutions of ammonia. This idea has received comparatively little attention since then. The group of A. D. King published a series of papers in the mid 1970s which summarize all previous work.[11] These workers reported the effects of pressure (from ∼1 to 60 atm) on the surface tension of water using a variety of "inert" pressurizing gases, including CO_2 and N_2O. Their results indicate adsorption and eventual condensation of the gas onto the water surface.

In a paper published in 1990, Jayne et al.[15] postulated the existence of a "chemisorbed" SO_2 species at the air−water interface, based on the kinetics of uptake of SO_2 into water droplets. Using a combination of surface second-harmonic generation and surface-tension measurements, we[3] provided direct evidence for the existence of an adsorbed S(IV) species at the air−aqueous interface of SO_2-containing solutions. Sulfur dioxide is but one example of a small, soluble, inorganic species exhibiting such behavior. In future papers we shall discuss several others of these; the present work is concerned with ammonia.

The paper is organized as follows. The following two sections present a thermodynamic and a kinetic framework, respectively, for analyzing the adsorption behavior of volatile solutes at the air−water interface. In section D, the experimental details of our measurements of equilibrium- and time-dependent surface tensions of ammonia solutions are presented. The experimental results are given in section E, followed by a description of ab initio methods used to model the NH_3−water interface in section F and by the ab initio results in section G. Section H concludes with a general discussion of the nature of ammonia adsorbed at the air−water interface.

B. Thermodynamics of Volatile Adsorbates

To understand the adsorption behavior of a volatile solute, X, it is necessary to consider its concentration in the gas, solution, and surface phases. (For thermodynamic completeness one should also consider the presence of air. However, its neglect does not lead to any significant errors under normal laboratory or atmospheric conditions.)[16] Denoting water as component 1 and X as 2, it can be shown[16] that the surface tension, σ, is given by

$$\sigma = f^{\sigma} - \sum_{i=1-2} \mu_i^{\sigma} \Gamma_i \qquad (1)$$

where f^{σ} is the surface Helmholtz free energy per unit area, A, μ_i^{σ} is the chemical potential of species i in the surface phase, $\mu_i^{\sigma} = \partial f^{\sigma}/\partial \Gamma_i$, and Γ_i is the surface excess of component i defined as $\Gamma_i = n_i^{\sigma}/A$. In general, the surface free energy function, f^{σ}, depends not only on the chemical potentials of all species in the surface phase, but also on their chemical potentials in the

10.1021/jp9833247 CCC: $18.00
Published on Web 12/10/1998

solution and gas phases. For this reason, the surface phase is said to be "nonautonomous". The dependence comes about physically because of interactions between molecules in the bulk phases adjacent to the interface with those in the surface phase, as well as interactions between molecules in the surface phase alone.

The surface free energy is thus a function of temperature and bulk and surface concentrations. The dependence on bulk concentrations (really, the activities) is expressed in terms of the form $\partial f^{\sigma}/\partial a_i^{aq} = \epsilon_i^{aq}$, where a_i^{aq} is the activity of species i in solution. The full differential of the surface tension is[16]

$$d\sigma = -s^{\sigma}dT - \sum_{i=1-2} \Gamma_i \, d\mu_i^{\sigma} - \sum_{i=1-2} \epsilon_i^{aq} \, da_i^{aq} - \sum_{i=1-2} \epsilon_i^{g} \, da_i^{g} \quad (2)$$

At equilibrium among all three phases, the chemical potential of each component is independent of phase and the ϵ's become zero.[16] Thus, *at equilibrium*, one obtains the common form of the Gibb's equation

$$d\sigma = -s^{\sigma} \, dT - \sum_{i=1-2} \Gamma_i \, d\mu_i^{\sigma} \quad (3)$$

Consideration of the phase rule for a planar interface leads to the conclusion that one cannot vary each of the four variables in the above expression independently; Γ_i cannot be measured simply as $\Gamma_i = (\partial\sigma/\partial\mu_i)_{T,\mu_j}$. What is actually measured are the *relative* adsorptions and *relative* surface entropies, $\Gamma_{1,i}$ and $(s^{\sigma})_1$, respectively. The adsorption of component i relative to component 1 (the solvent, water, in this case) is defined to be

$$\Gamma_{1,i} = \Gamma_i - \Gamma_1 \{(a_i^{aq} - a_i^{g})/(a_1^{aq} - a_1^{g})\} \quad (4)$$

This quantity is not only thermodynamically correct, but has the advantage that it is independent of the choice of dividing surface. It is straightforward then to show that $\Gamma_{1,i}$ is equivalent to Γ_i determined at the surface where $\Gamma_1 = 0$.[16] The relative surface coverage is then given by

$$\Gamma_{1,i} = (\partial\sigma/\partial\mu_i)_{T,\mu_j \neq 1} \quad (5)$$

The chemical potentials for species i in the bulk phases are

$$\mu_i^{g} = \mu_i^{\circ,g} + RT \ln(p_i/p^{\circ})$$
$$\mu_i^{aq} = \mu_i^{\circ,aq} + RT \ln(a_i/a^{\circ}) \quad (6)$$

where p° and a° are the standard pressure (1 atm) and standard activity (1 mol kg^{-1}), respectively. The activity, a_i, is given by $a_i = \gamma_i \, m_i$, where the γ_i are concentration-dependent activity coefficients and m_i represents the solute concentration in mol kg^{-1}. In eq 6 we have assumed ideal gas behavior of the vapor. For the surface phase, we use the standard state proposed by Kemball and Rideal.[17] By analogy to the gas-phase standard state, these authors argued that the standard state of an adsorbed film is a film with the same number density as would be present in an ideal gas at 1 atm in a container of thickness 6 Å. This amounts to setting a temperature-dependent area per molecule, in direct analogy to the temperature-dependent molar volume of an ideal gas. In terms of film pressure, π, defined as $\pi = \sigma^* - \sigma$, where σ^* is the surface tension of the pure solvent, the standard state is $\pi^{\circ} = 0.06084$ dyne cm^{-1}. This is independent of temperature, just as is the gas-phase standard state.

Hence, for the surface phase we have

$$\mu_i^{\sigma} = \mu_i^{\circ,\sigma} + RT \ln(\pi_i/\pi^{\circ}) \quad (7)$$

for an "ideal gas"-type film. This can be extended to include nonidealities by use of a surface activity coefficient, γ_i^{σ}, so that

$$\mu_i^{\sigma} = \mu_i^{\circ,\sigma} + RT \ln(\gamma_i^{\sigma}\pi_i/\pi^{\circ}) \quad (7a)$$

At phase equilibrium, the chemical potentials are all equal, $\mu_i^{g} = \mu_i^{\sigma} = \mu_i^{aq}$ and from eqs 5 and 6

$$\Gamma_{1,i} = (\partial\sigma/\partial\mu_i)_{T,\mu_j \neq 1} = -(a_i/RT)(\partial\sigma/\partial a_i) \quad (8)$$

for adsorption of species i from solution.

The free energy for transferring 1 mol of species i from solution to the surface (the molar free energy of adsorption) is

$$\Delta G_{aq\to\sigma} = \mu_i^{\sigma} - \mu_i^{aq} = (\mu_i^{\circ,\sigma} - \mu_i^{\circ,aq}) + RT \ln\{(\gamma_i^{\sigma}\pi_i/\pi^{\circ})/(a_i/a^{\circ})\}$$

At phase equilibrium, $\Delta G_{aq\to\sigma} = 0$ and we obtain

$$\Delta G^{\circ}_{aq\to\sigma} = -RT \ln\{(\pi_i/\pi^{\circ})/(a_i/a^{\circ})\}_{eq} \quad (9)$$

for an ideal-gas film and, in general,

$$\Delta G^{\circ}_{aq\to\sigma} = -RT \ln\{(\gamma_i^{\sigma}\pi_i/\pi^{\circ})/(a_i/a^{\circ})\}_{eq} \quad (9a)$$

This can be related to adsorption onto the surface from the vapor phase by transforming the solution activities to equilibrium vapor pressures via the Henry's Law constant, K_H: $p_i/p^{\circ} = (a_i/a^{\circ})/K_H$, so that

$$\Delta G^{\circ}_{g\to\sigma} = -RT \ln\{(\gamma_i^{\sigma}\pi_i/\pi^{\circ})/(p_i/p^{\circ})\}_{eq} \quad (10)$$

A plot of $RT \ln\{(\gamma_i^{\sigma}\pi_i/\pi^{\circ})/(p_i/p^{\circ})\}_{eq}$ vs (p_i/p°) extrapolated to zero pressure will yield the "ideal gas" value of $\Delta G^{\circ}_{g\to\sigma}$. Over a reasonable temperature range, the entropy and enthalpy of adsorption may be considered constant and can be calculated from the T-dependence of ΔG° determined above as

$$\Delta S^{\circ} = -(\partial\Delta G^{\circ}/\partial T) \text{ and } \Delta H^{\circ} = (\partial\Delta G^{\circ}/T)/\partial(1/T) \quad (11)$$

C. Adsorption Kinetics of Volatile Solutes

We will model the gas−surface−solution system as the species X which can exist in either of the bulk phases and can also occupy vacant surface sites, Σ: $X^{aq} + \Sigma \rightleftarrows X^{\sigma} \rightleftarrows X^{g} + \Sigma$. This gives rise to the equations

$$(d/dt)[X^{aq}] = -k_1[X^{aq}][\textstyle\sum] + k_{-1}[X^{\sigma}]$$
$$(d/dt)[X^{\sigma}] = k_1[X^{aq}][\textstyle\sum] - k_{-1}[X^{\sigma}] + k_2[X^{g}][\textstyle\sum] - k_{-2}[X^{\sigma}]$$
$$= (k_1[X^{aq}] + k_2[X^{g}])[\textstyle\sum] - (k_{-2} + k_{-1})[X^{\sigma}]$$
$$(d/dt)[\textstyle\sum] = -(d/dt)[X^{\sigma}]$$
$$(d/dt)[X^{g}] = -k_2[X^{g}][\textstyle\sum] + k_{-2}[X^{\sigma}] \quad (12)$$

The total concentration of surface adsorption sites is $N = [\Sigma] + [X^{\sigma}]$, and so the relative coverage, $\Theta = [X^{\sigma}]/N$ and $[X^{\sigma}] = N\Theta$; $[\Sigma] = (1 - \Theta)N$. In terms of Θ we obtain for the time dependence of the coverage

$$(d/dt)\Theta = -(k_{-1} + k_{-2} + k_1[X^{aq}] + k_2[X^g])\Theta + k_1[X^{aq}] + k_2[X^g] \quad (13)$$

In general, both $[X^{aq}]$ and $[X^g]$ are time dependent, making a straightforward solution for $\Theta(t)$ difficult.

At equilibrium among all phases, $(d/dt)\Theta = 0$ and so

$$\Theta_{eq} = \frac{k_1[X^{aq}] + k_2[X^g]}{k_{-1} + k_{-2} + k_1[X^{aq}] + k_2[X^g]} \quad (14)$$

Since at equilibrium, $[X^{aq}] = K_H[X^g]$, we can write

$$\Theta_{eq} = \frac{(k_1 + K_H^{-1}k_2)[X^{aq}]}{(k_{-1} + k_{-2}) + (k_1 + K_H^{-1}k_2)[X^{aq}]} = \frac{[X^{aq}]}{\frac{(k_{-1} + k_{-2})}{(k_1 + K_H^{-1}k_2)} + [X^{aq}]} \quad (15)$$

which is cast in the form of a Langmuir adsorption isotherm[18]

$$\Theta = \frac{[X^{aq}]}{b + [X^{aq}]} \quad (16)$$

where

$$b = \frac{k_{-1} + k_{-2}}{k_1 + K_H^{-1}k_2} \quad (17)$$

If the solute is nonvolatile so the vapor−surface equilibrium can be ignored, b is simply the inverse of the adsorption equilibrium constant from solution

$$(K^{\sigma,aq})^{-1} = k_{-1}/k_1 \quad (18)$$

Similarly, for insoluble adsorbates, b is related to the gas−surface equilibrium constant. However, when all three phases are important, b is as given in eq 17. Under these conditions, it is the *total* flux to and from the interface, from the gas phase and from the solution phase, which determines the equilibrium surface coverage. Care should therefore be taken to include the flux from solution when applying arguments of detailed balance to estimate the surface coverage of atmospheric droplets.

If the system is not at true equilibrium but consists of an aqueous solution of X which is open to the atmosphere, X will evaporate from the surface and leave the system. If this is the case, the gas-phase concentration remains negligible so adsorption from the vapor phase may safely be neglected. Under these conditions, eq 13 can be approximated in two limits. If the rate of evaporation is small and rate-determining in the time dependence of the coverage, the solution and surface phases are close to equilibrium and we may approximate the ϵ_i terms in eq 2 to be zero. Then $k_1/k_{-1} \approx K^{\sigma,aq}$, so $[X^{\sigma}] = K^{\sigma,aq}[X^{aq}][\Sigma]$ and therefore $\Theta/(1 - \Theta) = K^{\sigma,aq}[X^{aq}]$. The resulting expression for the time dependence of the coverage is

$$(d/dt)\Theta \approx -k_{-2}K^{\sigma,aq}[X^{aq}]/(1 + K^{\sigma,aq}[X^{aq}]) \quad (19)$$

This suggests that if the assumptions given above hold and the bulk concentration does not change over the course of the experiment, $\Theta(t)$ is a simple linear function of time. Since we have approximated the ϵ_i terms in eq 2 to be zero in this case, $\Theta(t)$ may be derived from measurements of the time-dependent surface tension using eq 8 to obtain $\Gamma_{1,X}(t)$ and setting $\Theta(t) = \Gamma_{1,X}(t)/\Gamma^{sat}{}_{1,X}$, where $\Gamma^{sat}{}_{1,X}$ is the relative surface excess of X at saturation of the surface.

The second limit will be approached when the time dependence of the surface coverage is determined by the population of the surface phase from the solution phase. This implies that evaporation is facile compared to transport of X from the bulk solution to the interface, suggesting that an energetic barrier exists along the reaction pathway for X proceeding from solution phase to the surface phase. Here we may no longer assume the ϵ_i terms in eq 2 to be zero, since there is no equilibrium between the surface and solution phases. In this case, surface-tension measurements do not directly yield the surface coverage. However, if the ϵ_i terms are assumed to be very small, the coverage is predicted to decay to some steady-state value (after some induction time) which depends on the solution concentration

$$\Theta_{ss} = \frac{k_1[X^{aq}]}{k_1[X^{aq}] + k_{-1} + k_{-2}} \quad (20)$$

which reduces to

$$\Theta_{ss} \approx k'[X^{aq}] \quad (20a)$$

if $k_1[X^{aq}] \ll (k_{-1} + k_{-2})$. Since we are assuming a vapor-phase concentration of zero, this requires that $\epsilon_i{}^{aq} \approx 0$, which is probably reasonable for low ionic strength solutions. When this is the case, measurements of the time dependence of the surface tension can distinguish between the two possibilities for rate-determining behavior. If a barrier exists on the reaction pathway between the adsorbed and the fully solvated states, we expect to measure a steady state in surface coverage. When there is no such barrier and evaporation from the surface is rate-determining, the rate constant for evaporation, k_{-2}, may be determined.

D. Experimental Methods

Static surface tensions of aqueous ammonia solutions were measured using both a DuNouy tensiometer and the capillary rise method.[19] The capillary rise method yields the surface tension when an equilibrium between vapor, solution, and surface phases exists. A capillary with an inner diameter of 0.0392 cm was used in a sealed vessel of diameter 2.8 cm. Measurements were performed in a commercial recirculating water bath with a stated temperature stability of ±0.2 K. The equilibrium surface tensions were measured at 278 and 298 K using this technique.

The time dependence of the surface tension was measured using the DuNouy tensiometer with a Pt ring of diameter 17.7 mm. These measurements were made at room temperature in an open container placed in a fume hood. This arrangement allowed vapor-phase ammonia to be removed from the 3-phase system as it was formed. The time dependence of the pH for several of these solutions was measured at the same time to monitor the time dependence of the bulk $[NH_3]$. The bulk concentration was also determined before and after each run by titration against a standardized HCl solution.

Solutions were prepared volumetrically from a stock 30 wt % ammonia solution. The actual NH_3 concentrations were determined by titration against a standardized HCl solution.

E. Experimental Results

(i) Ammonium Hydroxide Solutions. In aqueous solution, ammonia is hydrolyzed to ammonium hydroxide $NH_3 + H_2O$

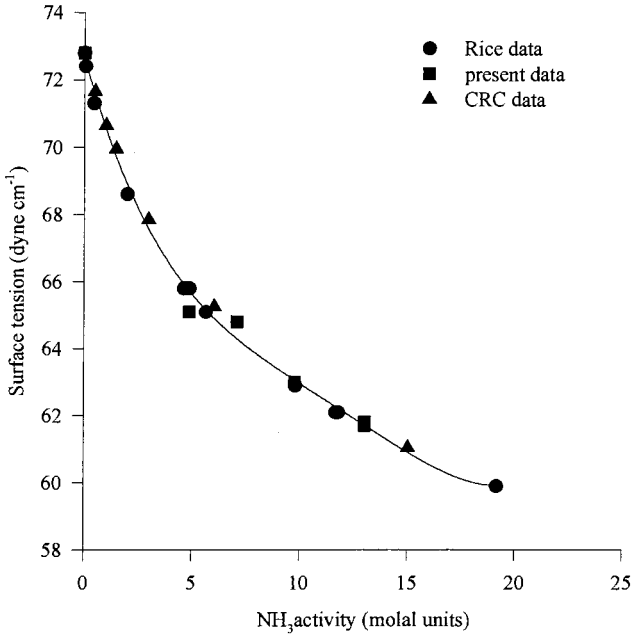

Figure 1. Surface tension at 298 K as a function of ammonia activity, calculated as described in the text. Results from Rice[7] (●), CRC[22] (▲), and present work (■) are shown. The line is a third-order polynomial fit to the data.

TABLE 1: Parameters[a] Used To Calculate Ammonia Activity and Vapor Pressure

$\gamma_{NH_3} = \exp(2m_{NH_3}\lambda)$, where $\lambda = 0.033161 - 21.12816/T + 4665.1461/T^2$
$\ln K_H = -8.09694 + 3917.507/T - 0.00314T$

[a] From ref 21.

$\rightleftarrows NH_4^+ + OH^-$ with an equilibrium constant[20] (at 298 K) of 1.774×10^{-5}. This is small enough that under all of the experimental conditions here, $[NH_3(aq)] + [NH_4^+(aq)] \approx [NH_3(aq)]$. (The least concentrated solutions of interest here have $m_{NH_3} \approx 0.5$ mol kg^{-1} and $[NH_4^+]/[NH_3] \approx 10^{-2}$.) The activity coefficient of the neutral NH_3 is both temperature- and concentration-dependent, however, and so the activity, $a_{NH_3} = \gamma_{NH_3} m_{NH_3}$, must be calculated for each concentration and temperature used. Clegg and Brimblecombe[21] provide parameters for evaluating γ_{NH_3} as a function of m_{NH_3} and T over the concentration and temperature ranges employed here. These are reproduced in Table 1.

At equilibrium, the vapor pressure of ammonia is related to its solution activity by the Henry's Law constant, K_H. We use the value for K_H and its temperature dependence given by Clegg and Brimblecombe.[21] Table 1 includes the Henry's Law constants used in the present work.

(ii) Equilibrium Surface-Tension Measurements. In a paper in 1928, O. K. Rice[7] reported the surface-tension depression of aqueous solutions of ammonia as a function of the wt % ammonia at 298 K. The concentrations given there were converted to molality units, and the activity coefficients were evaluated using the parameters given in Table 1. This allows calculation of the equilibrium partial pressure of NH_3 above the solution as well, via the Henry's Law constant. Figure 1 displays the surface tension of ammonia solutions as a function of the solution-phase activity. Data from Rice,[7] the CRC Handbook,[22] and our present 298 K results are included. The data are fit to a third-order polynomial function. Other types of functions may be used and give comparable fits to the data. Γ_{1,NH_3} is then given by eq 8

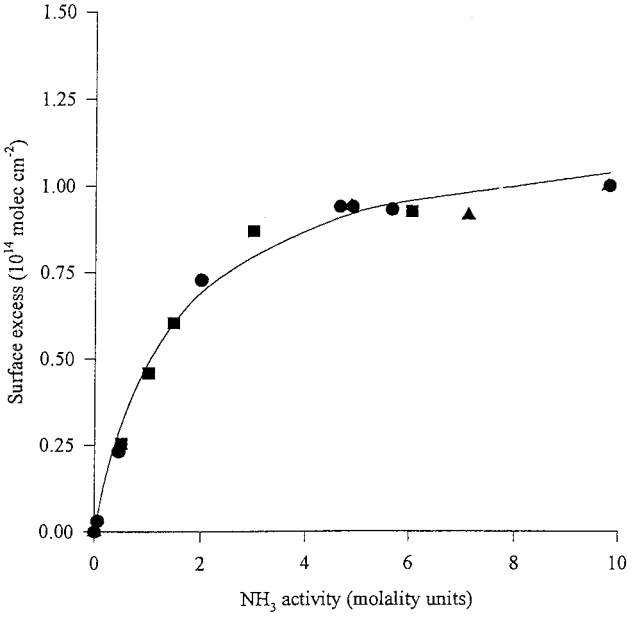

Figure 2. Ammonia surface excess at 298 K as a function of ammonia solution activity. The line shows a fit of the data to a Langmuir adsorption isotherm. The symbols are as given in Figure 1.

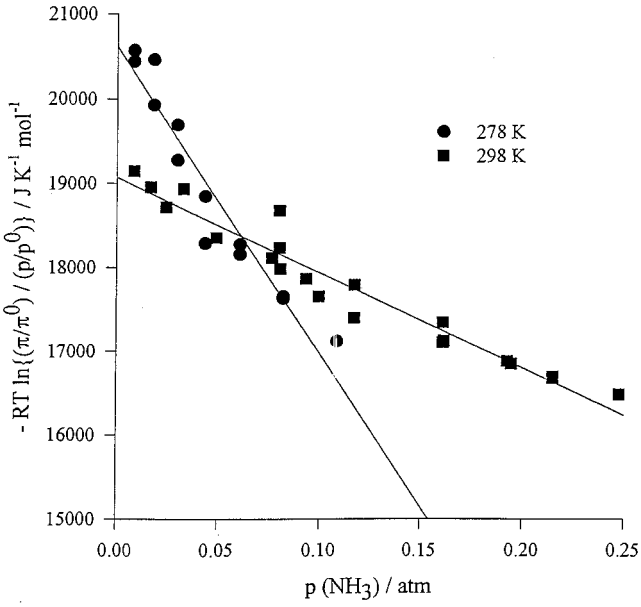

Figure 3. Plots of eq 10 to extract $\Delta G°$ for adsorption of ammonia from the gas phase onto the water surface. Data for 278 K (●) and 298 K (■) are shown. The lines are fits of the data to linear functions of ammonia pressure.

$$\Gamma_{1,NH_3} = -(a_{NH_3}/RT)(\partial\sigma/\partial a_{NH_3})_T$$

Figure 2 shows a plot of the relative surface adsorption of ammonia as a function of its activity in solution. Fitting this to a Langmuir isotherm, as in eq 15,

$$\Theta = \Gamma_{1,NH_3}/\Gamma^{sat}_{1,NH_3} = a_{NH_3}/(a_{NH_3} + b)$$

we obtain the saturated coverage to be $\Gamma^{sat}_{1,NH_3} = (1.19 \pm 0.05) \times 10^{14}$ molecules cm^{-2} and the value of b in eq 17 to be 1.43 $\pm$ 0.22 m. We estimate the true uncertainty in Γ^{sat}_{1,NH_3} to be of the order of 20%, based upon the different values obtained using different functions to fit the data shown in Figure 1.

Figure 3 shows plots of $RT \ln\{(\gamma^\sigma \pi_{NH_3}/\pi°)/(p_{NH_3}/p°)\}_{eq}$ vs the equilibrium vapor pressure of ammonia (as suggested by

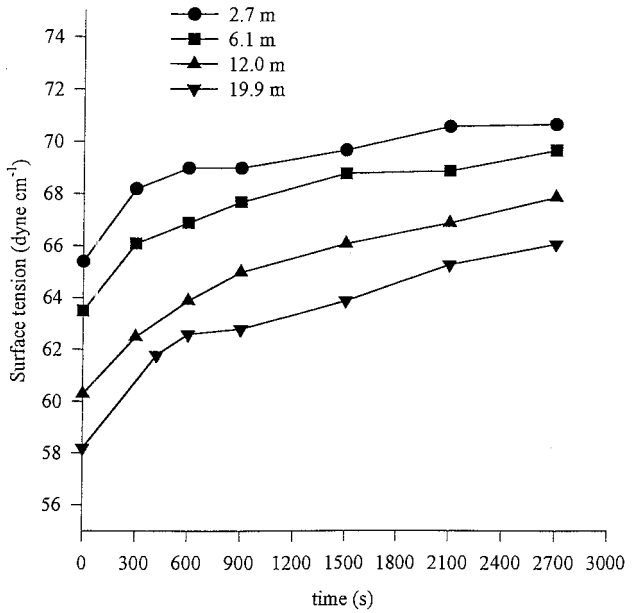

Figure 4. Surface tension as a function of time for uncovered ammonia solutions at 298 K. Several initial bulk concentrations are shown. The lines are present merely to guide the eye.

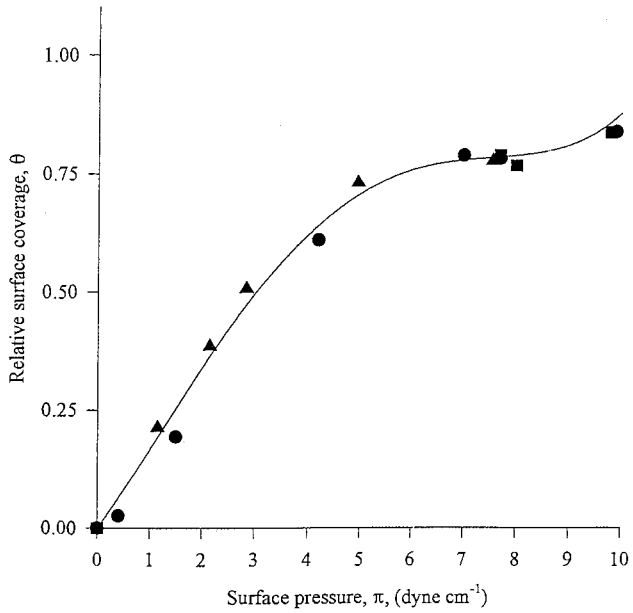

Figure 5. Ammonia surface coverage as a function of its surface pressure. See text for details.

eq 10) at two temperatures. The 298 K data include the results of Rice,[7] those reported in CRC,[22] and our own experimental values. The 278 K data are those measured in the present study. There is some pressure dependence on $\Delta G°$ calculated this way, which reflects the pressure dependence of the surface activity coefficient. (This comes from the vapor pressure dependence of the surface coverage and, hence, the surface pressure.) Extrapolating the curves to $p = 0$, we obtain a value for the standard free energy of adsorption from the gas phase to be $-(19.1 \pm 0.5)$ kJ mol^{-1} at 298 K and $-(20.6 \pm 0.5)$ kJ mol^{-1} at 278 K. These values yield a calculated entropy of adsorption from the gas phase of $-(75 \pm 50)$ J K^{-1}mol^{-1} and a calculated enthalpy of adsorption from the gas phase of $-(41 \pm 5)$ kJ mol^{-1}.

(iii) Time-Dependent Surface-Tension Measurements. The time dependence of the surface tension of several concentrations of ammonia solution, measured in an open container at room temperature, is illustrated in Figure 4. Solutions at all concentrations show a monotonic increase in the surface tension with time, from an initial value very close to the equilibrium surface tension to a value appropriate for water after several hours. Since adsorption of surface-active contaminants would necessarily decrease the surface tension, the observed increase is interpreted as being due to the loss of ammonia from the interface. This behavior suggests that the surface coverage of NH_3 does not achieve a steady state, as predicted by eq 20, and so the quasi-equilibrium assumptions used to derive eq 19 could be valid under the present conditions. In this case, the surface tension can be related to a surface coverage, via the fitting functions shown in Figures 1 and 2. For convenience, the surface tension is transformed to a surface pressure, π; a plot of $\Theta = \Gamma/\Gamma^{sat}$ vs π is displayed in Figure 5, with a fourth-order polynomial fit (for interpolation) also shown. Using this function, the surface tension vs time data may be transformed into surface coverage vs time. Figure 6 illustrates several representative Θ vs time plots obtained using this procedure.

This plot shows a linear dependence of the relative surface coverage on time for all concentrations, as implied by eq 19 above. In total, five concentrations with solution activities below 12 *m* and five with activities 15−28 *m* were used. To ensure

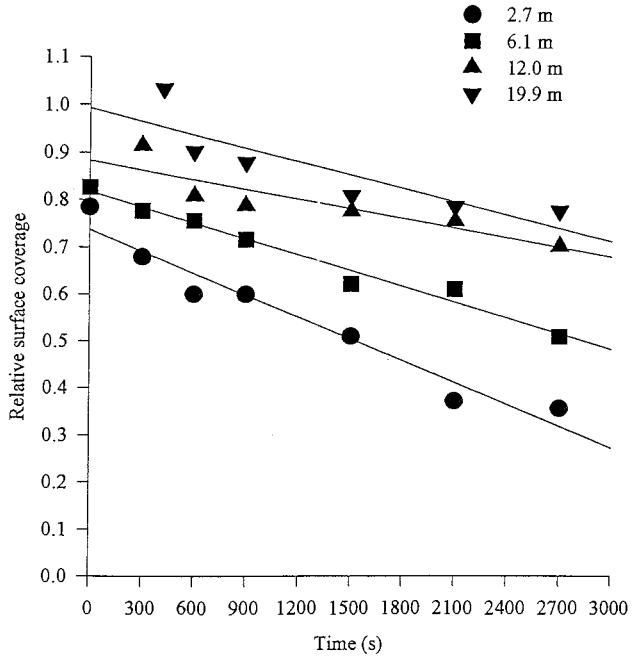

Figure 6. Ammonia surface coverage as a function of time. Symbols are the same as those for Figure 4. The lines show linear fits to the decays.

that the assumption of constant bulk concentration is valid, the solution pH was monitored over the course of the experiment for several of the solutions. In addition, the $[NH_3]$ was determined before and after the experiment by titration. Over the course of a 1-h measurement, the bulk concentration decreases by less than 20%, as determined by both these methods.

If we approximate $K^{\sigma,aq} \approx 1/b$ from eq 18, then the results displayed in Figure 2 give $K^{\sigma,aq} \approx 0.70$. Multiplying the slopes of the coverage vs time plots shown in Figure 6 by a factor of $-(1 + K^{\sigma,aq}[X^{aq}])/K^{\sigma,aq}[X^{aq}]$ yields values of k_{-2}, as long as eq 19 holds. There is a slight decrease in the k_{-2} extracted in this way as the bulk concentration increases. At lower bulk concentrations, corresponding to lower initial surface coverages, k_{-2} decreases from about 3×10^{10} s^{-1} when the solution phase

activity of ammonia is 1−2 molal, to about one-half that value at solution activities of ∼15 molal. At the higher concentrations, with solution-phase activities greater than approximately 15 molal, the k_{-2} values lie in the range $(4-8) \times 10^9$ s^{-1}.

Assuming that the evaporation rate constant is given by the transition-state theory expression

$$k_{-2} = \frac{k_B T}{h} e^{-\Delta G^{\ddagger}/(k_B T)}$$

where k_B and h represent Boltzmann's and Planck's constants, respectively, we obtain an activation free energy for evaporation of ammonia from the surface; $\Delta G^{\ddagger} = 13-15$ kJ mol^{-1} from the rates measured using the lower solution concentrations and $\Delta G^{\ddagger} = 16-18$ kJ mol^{-1} for the higher bulk concentrations.

F. Ab Initio Studies

(i) Defining the Problem. To gain some understanding of the molecular-level forces responsible for the adsorption of NH_3 at the air−water interface, we performed ab initio calculations to obtain structural and energetic parameters of the species expected to be important. A strong hydrogen bond is formed between ammonia and water. A priori, then, we anticipate that the binding of ammonia to the water surface occurs via hydrogen bonding to the fraction of water molecules with "dangling" O−H bonds at the interface. The simplest model for such binding is the water−ammonia dimer, NH_3-H_2O. Because inductive or cooperative effects may also occur in hydrogen bonding, especially when a cyclic species may be formed,[23] we performed calculations on the $NH_3-(H_2O)_2$ complex as well. Since the concentration of dangling O−H bonds at the interface is not large, these two models are expected to capture most of the important features of the binding to the surface.

(ii) Ab Initio Methods. All calculations were performed using the GAUSSIAN 94W suite of programs [24] on a Pentium II based computer. The basis sets used were the standard split-valence sets available in the program suite. Geometry optimizations of all species were carried out at the MP2 level using the 6-31G-(d,p) basis set. The energetics of the $NH_3 + H_2O \rightarrow NH_3-H_2O$ and the $2H_2O \rightarrow (H_2O)_2$ reactions were calculated at the MP4(SDTQ)/6-311++G(3df,2pd) level; for the $NH_3 + (H_2O)_2 \rightarrow NH_3-(H_2O)_2$ reaction, energies were calculated at the MP4-(SDTQ)/6-311+G(2d,p) level.

At all the calculated stationary points, vibrational frequency calculations were performed to ensure that these were true minima. These determinations were done at the MP2/6-31G-(d,p) level by analytical calculation of the harmonic force constants at the stationary point. Since calculations of this type typically overestimate the harmonic force constants, the calculated harmonic frequencies were corrected by the factor 0.9427.[25]

The basis-set superposition errors (BSSE)[26] in the calculations involving complexes were estimated using the full counterpoise correction.[27] At the optimum geometry of each complex, the total energy was calculated using "ghost" orbitals on each partner in the complex in turn. The difference between this energy and the energy of the isolated species gives the artificial lowering of the energy by the presence of the basis functions on the other partner. For example, the water nuclear charges are set to zero in the NH_3-H_2O complex and the energy calculated; the result gives the lowering of the ammonia energy by the presence of the basis functions on water. This energy, labeled $E(NH_3(H_2O)^{gh})$, is subtracted from $E(NH_3)$ to give the BSSE estimate for ammonia in the complex, $BSSE_{NH_3}$. The binding energy of the complex is then calculated to be, for example in the NH_3-H_2O case, $\Delta E = E(NH_3-H_2O) - E(NH_3) - E(H_2O) - BSSE_{NH_3} - BSSE_{H_2O}$.

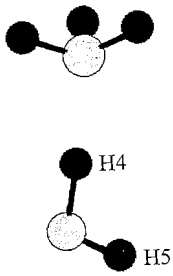

Figure 7. Structure of the NH_3-H_2O complex, calculated ab initio. Geometric parameters are given in Table 2. Note that this and the structure illustrated in Figure 8 are projections of the full three-dimensional structures. The full structural parameters of each complex are available from the author on request.

TABLE 2: Geometry of the NH_3-H_2O Complex[a]

$r(N-H_{1-3}) = 1.013$ Å	$\angle(H-N-H) = 106°$
$r(N-H_4) = 1.991$ Å	
$r(N-O) = 2.961$ Å	$\angle(N-H_4-O) = 175°$
$r(O-H_4) = 0.972$ Å	
$r(O-H_5) = 0.960$ Å	$\angle(H_5-O-H_4) = 104°$

[a] Numbering on H atoms from Figure 7.

TABLE 3: Calculated (Experimental)[a] Rotational and Vibrational Constants for $NH_3 + H_2O \rightarrow (NH_3-H_2O)$

	NH_3	H_2O	(NH_3-H_2O)
	Rotational Constants (cm^{-1})		
A	9.926 (9.944)	26.78 (27.88)	4.935 (4.927)
B	9.882 (9.944)	14.62 (14.51)	0.208 (0.206)
C	6.398 (6.196)	9.46 (9.28)	0.202 (0.204)
	Scaled Harmonic Vibrational Frequencies (cm^{-1})		
	3505 (3443)	3676 (3657)	3505; 3514
	3358 (3337)	3806 (3756)	3360; 3758
	1627 (1627)	1585 (1595)	1640, 1623; 1615
	1059 (968)		1091
			664 (662)
			429 (411)
			189 (202)
			158 (180)
			149
			25 (19)

[a] Constants for molecules from Herzberg,[37] for complex from ref 32.

G. Ab Initio Results

(i) The Reaction $NH_3 + H_2O \rightarrow NH_3-H_2O$. The (NH_3-H_2O) complex has been studied both experimentally, by microwave and far-infrared spectroscopy,[28−31] and theoretically, by ab initio calculations.[32,33] It is bound by a hydrogen bond between an H atom of the water moiety and the lone pair on the N atom of ammonia. The vibrationally averaged N−O distance is determined to be 2.98 Å from the microwave data[30] and 2.93−3.05 Å by ab initio calculation,[33] depending on the level of calculation used. The hydrogen bond is somewhat nonlinear, with an NHO bond angle estimated to be ∼10° by experiment[30] and about 5−6° by calculation.[33]

The optimized geometry found in the present calculation, at the MP2/6−61G(d,p) level, is given in Table 2 and illustrated in Figure 7. Table 3 gives our calculated rotational and vibrational frequencies for the reagents and the complex, also at the MP2/6-31G(d,p) level. The agreement with experiment and with previous calculations[32−34] is very good.

TABLE 4: Energetics for $NH_3 + H_2O \rightarrow NH_3{-}H_2O$

	MP4SDTQ/ 6-311+G- (2d,p)	MP4SDTQ/ 6-311++G- (3df,2pd)	QCISD(T)/ 6-311++G- (3df,2pd)
H_2O[a]	−76.30250	−76.33772	−76.33672
NH_3[a]	−56.44629	−56.47648	−56.47627
$NH_3{-}H_2O$[a]	−132.75978	−132.82475	−132.82346
$(NH_3)^{gh}{-}H_2O$[a]	−76.30304	−76.33809	
$NH_3{-}(H_2O)^{gh}$ [a]	−56.44753	−56.47706	
ΔE[b]	−28.83	−27.70	−27.50
BSSE[b]	+4.65	+2.47	
ΔE (BSSE corrected)[b]	−24.19	−25.24	
zero-point correction[b]	+8.83	+8.83	
$\Delta E_0°$ [b]	−15.48	−16.32	

[a] Energies in Hartrees. [b] Energies in kJ mol^{-1}.

The energies of the complex and the reagents as well as the counterpoise correction were calculated at the MP4 level using both a 6-311+G(2d,p) and the large 6-311++G(3df,2pd) basis set at the MP2/6-61G(d,p) optimized geometries. The reagent and complex energies (but not the counterpoise correction) were also calculated at the QCISD(T)/6-311++G(3df,2pd)//MP2/6-31G(d,p) level. The results of these calculations and the derived thermochemistries are shown in Table 4.

The total calculated binding energy for the complex (not BSSE-corrected) is essentially the same at the MP4 and QCISD-(T) levels using the large basis set, suggesting that the MP4 energetics given here reflect most or all of the correlation effects in the binding. As expected, the BSSE calculated at the MP4 level is significantly larger for the smaller basis set than for the larger one. However, the total binding energy is also calculated to be larger; the result is that the BSSE-corrected binding energy at the MP4 level is essentially the same for the two basis sets.

Taking a BSSE- and ZPE-corrected binding energy of $\Delta E_0° = -16.3$ kJ mol^{-1} and the rotational and vibrational frequencies listed in Table 3, partition functions may be calculated for the reagents and complex. This allows calculation of the equilibrium constant for formation of the dimer as well as the standard free energy, enthalpy, and entropy of its formation from water and ammonia. We find $\Delta H° = -18.4$ kJ mol^{-1} and $\Delta S° = -91$ J K^{-1} mol^{-1}, giving a 270 K value for $\Delta G°$ of +6.2 kJ mol^{-1} and $K_p(270) = 0.063$ (atm^{-1}). This suggests that the 1:1 complex may play some role in the atmospheric chemistry of NH_3, especially under very humid conditions.

To estimate the thermochemistry of binding to a water surface, we take $\Delta H°$ to be the same as that for 1:1 complex formation and calculate the entropy of adsorption to the surface. Following Adamson,[18] we estimate the adsorption entropy as $\Delta S°_{ads} = (S^{°,\sigma}{}_{config} + S^{°,\sigma}{}_{trans,2-D} + S^{°,\sigma}{}_{internal}) - S^{°,g}$, where the terms in the parentheses represent the configurational, translational, and internal contributions to the entropy of the adsorbed species, respectively, and the standard entropy of gas-phase ammonia is designated $S^{°,g}$. The standard configurational entropy is given by $S^{°,\sigma}{}_{config} = -R\ln(\Theta°/(1-\Theta°))$ and the standard translational entropy is that of a particle in a 2-D box having the same area as that occupied by the adsorbed species in its standard state. Recalling that we have chosen the standard state to have $\pi° = 0.06084$ dyne cm^{-1} (and, correspondingly, an area per molecule of 22.53 Å^2),[17] we obtain from the fit in Figure 5 $\Theta° \approx 0.01$, so $S^{°,\sigma}{}_{config} = 38.3$ J K^{-1} mol^{-1} and $S^{°,\sigma}{}_{trans,2-D} = 104.9$ J K^{-1} mol^{-1}. We estimate the standard internal entropy of the adsorbed species as the difference between the vibrational entropy of the 1:1 complex and the vibrational entropy of water. This procedure gives a value of 58.2 J K^{-1} mol^{-1} for $S^{°,\sigma}{}_{internal}$.

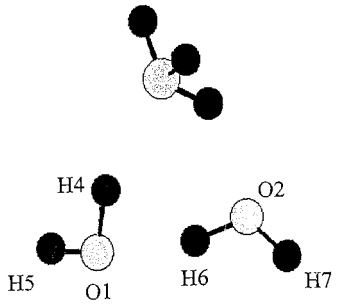

Figure 8. Structure of the $NH_3{-}(H_2O)_2$ complex, calculated ab initio. Geometric parameters are given in Table 5.

TABLE 5: Geometry of the $NH_3{-}(H_2O)_2$ Complex[a]

$r(N{-}H_{1-3}) = 1.012$ Å	$\angle(H{-}N{-}H) = 107°$
$r(N{-}H_4) = 1.888$ Å	
$r(N{-}O_1) = 2.816$ Å	$\angle(N{-}H_4{-}O_1) = 181°$
$r(O_1{-}H_4) = 0.983$ Å	
$r(O_1{-}H_5) = 0.962$ Å	$\angle(H_5{-}O{-}H_4) = 105°$
$r(N{-}O_2) = 3.036$ Å	
$r(O_1{-}O_2) = 3.079$ Å	
$r(O_1{-}H_6) = 1.880$ Å	
$r(O_2{-}H_5) = 0.962$ Å	
$r(O_2{-}H_6) = 0.975$ Å	$\angle(H_6{-}O_2{-}H_7) = 104°$
$r(O_2{-}H_7) = 0.961$ Å	

[a] Numbering on H atoms from Figure 8.

TABLE 6: Calculated Rotational and Vibrational Constants for $(H_2O)_2$ and $NH_3{-}(H_2O)_2$

	$(H_2O)_2$	NH_3-$(H_2O)_2$
	Rotational Constants (cm^{-1})	
A	7.49	0.236
B	0.212	0.195
C	0.212	0.111
	Scaled Harmonic Vibrational Frequencies (cm^{-1})	
	3773; 3752	3746; 3736; 3506
	3641; 3572	3491; 3465; 3349; 3310
	1564; 1544	1653; 1640; 1629; 1612
		1138
	638; 351; 191	921; 698; 481; 437
	169; 161; 136	386; 272; 231; 217
		203; 197; 161; 149

The calculated value of $S^{°,g}$ using the parameters in Table 5 is 200.9 J K^{-1} mol^{-1}, yielding a calculated adsorption entropy of ~0 J K^{-1} mol^{-1}. The calculated $\Delta G°_{ads}$ becomes ca. −18 kJ mol^{-1}.

(ii) The Reaction $NH_3 + (H_2O)_2 \rightarrow NH_3{-}(H_2O)_2$. The $NH_3{-}(H_2O)_2$ complex has not, to our knowledge, been reported previously, either experimentally or theoretically. The geometry, optimized at the MP2/6-31G(d,p) level, is given in Table 5 and illustrated in Figure 8. This is, of course, one of several potential minima on the full $NH_3{-}(H_2O)_2$ potential energy hypersurface. We believe it to be the global minimum of this system. The rotational and vibrational constants of the reagents and the complex are listed in Table 6. Energetics calculated at the MP4/6-311+G(2d,p)//MP2/6-31G(d,p) level for the reactions $2H_2O \rightarrow (H_2O)_2$ and $NH_3 + (H_2O)_2 \rightarrow NH_3{-}(H_2O)_2$ are given in Table 7. At the MP4/6-311++G(3df,2pd)//MP2/6-31G(d,p) level, the BSSE- and ZPE-corrected binding energy for the water dimer is −12.2 kJ mol^{-1}, in good agreement with calculations and experimental estimates.[35]

The BSSE- and ZPE-corrected binding energy of NH_3 to the water dimer is calculated to be −24.9 kJ mol^{-1}. The total interaction energy was determined to be equal to the sum of the three two-body interactions between the complex partners. We conclude that the binding is due to the formation of two

TABLE 7: Energetics for $2H_2O \rightarrow (H_2O)_2$ and $NH_3 + (H_2O)_2 \rightarrow NH_3-(H_2O)_2$

	MP4SDTQ/ 6-311+G(2d,p)	MP4SDTQ/ 6-311++G(3df,2pd)
H_2O[a]	−76.30250	−76.33772
NH_3[a]	−56.44629	−56.47648
$(H_2O)_2$[a]	−152.61424	−152.68369
$NH_3-(H_2O)_2$[a]	−209.07703	
$(H_2O)^{gh}-H_2O$[a]	−76.30393	−76.33827
$H_2O-(H_2O)^{gh}$ [a]	−76.30250	−76.33801
$(NH_3)^{gh}-(H_2O)_2$[a]	−152.61403	
$NH_3-(H_2O)_2^{gh}$ [a]	−56.44787	
	$2H_2O \rightarrow (H_2O)_2$	
ΔE[b]	−24.26	−21.66
BSSE[b]	+3.7	+1.44
ΔE(BSSE corrected)[b]	−20.56	−20.22
zero-point correction[b]	+8.29	+8.29
ΔE_0° [b]	−12.27	−11.93
	$NH_3 + (H_2O)_2 \rightarrow NH_3-(H_2O)_2$	
ΔE[b]	−43.35	
BSSE[b]	+4.18	
ΔE(BSSE corrected)[b]	−39.17	
zero-point correction[b]	+14.23	
ΔE_0° [b]	−24.94	

[a] Energies in Hartrees. [b] Energies in kJ mol^{-1}.

TABLE 8: Summary of Thermochemistry at 298 K

Experimental Results

$\Delta H_{soln} = -34.0$ kJ mol^{-1}	$\Delta H^\circ_{ads} = -(41 \pm 5)$ kJ mol^{-1}
$\Delta S_{soln} = -80$ J K^{-1} mol^{-1}	$\Delta S^\circ_{ads} = -(75 \pm 50)$ J K^{-1} mol^{-1}
$\Delta G_{soln} = -10.2$ kJ mol^{-1}	$\Delta G^\circ_{ads} = -(19.1 \pm 0.5)$ kJ mol^{-1}
	$\Delta G^\ddagger_{evap} = +(13 - 18)$ kJ mol^{-1}

ab Initio Results

1:1 complex	1:2 complex
$\Delta H^\circ_{ads} = -18.4$ kJ mol^{-1}	$\Delta H^\circ_{ads} = -29.8$ kJ mol^{-1}
$\Delta S^\circ_{ads} = \sim 0$ J K^{-1} mol^{-1}	$\Delta S^\circ_{ads} = -33.7$ J K^{-1} mol^{-1}
$\Delta G^\circ_{ads} = -18$ kJ mol^{-1}	$\Delta G^\circ_{ads} = -19.8$ kJ mol^{-1}

hydrogen bonds and that contributions from cooperative effects[23] are minimal. As was done for the 1:1 complex, we calculate the partition functions and thus values for the standard free energy, enthalpy, and entropy for the reaction forming $NH_3-(H_2O)_2$ from ammonia and the water dimer. The calculation yields −29.8 kJ mol^{-1} for ΔH° and $\Delta S^\circ = -152$ J K^{-1} mol^{-1}. These values are such that this reaction is unlikely to be atmospherically important. Combining them with the ΔH° and ΔS° calculated for the 1:1 complex formation, we obtain the free energy change for the reaction $2H_2O + NH_3 \rightarrow NH_3-(H_2O)_2$. At 270 K, $\Delta G^\circ = +17.4$ kJ mol^{-1} for this process and the equilibrium constant is therefore 4.3×10^{-4} atm^{-2}. We conclude that the ammonia−water dimer complex is probably not important in the atmosphere.

By following the procedure outlined above for the 1:1 complex, we again calculate the entropy and free energy of adsorption of ammonia on water, but now assuming the important features of the interaction are captured by the $NH_3-(H_2O)_2$ complex. The calculated standard configurational and translational entropies are the same in this case as those given above. The calculated $S_{internal}^\circ$ is now 24.2 J K^{-1} mol^{-1}, giving a calculated ΔS_{ads}° of −33.7 J K^{-1} mol^{-1}. These results are listed with those corresponding to the 1:1 complex in Table 8, which also displays the experimentally obtained thermochemistry.

H. Discussion

The combined results shown in Table 8 paint an interesting picture of the ammonia−water interaction. A comparison of the thermochemistry derived from the equilibrium surface-tension measurements with that of full solvation of NH_3 in water suggests that ammonia is almost fully solvated in its surface-bound state. Both the standard enthalpy and standard entropy of adsorption from the gas phase are close to the corresponding values of ΔH_{soln}° and ΔS_{soln}°, although there are significant uncertainties in the adsorption results. The standard free energy of adsorption is somewhat better determined here; its magnitude implies that the surface-bound standard state lies approximately 10 kJ mol^{-1} below the standard state of the fully solvated species in the temperature range 270−300 K.

The saturated coverage derived from the equilibrium surface-tension measurements is $(1.2 \pm 0.2) \times 10^{14}$ molecules cm^{-2}. This is close to the estimated surface density of "free" O−H groups reported by Shen and co-workers[36] of 2×10^{14} molecules cm^{-2} (assuming a surface density of water of 1.04×10^{15} molecules cm^{-2}). This result implies that there is at most one adsorbed ammonia per free OH in the surface-bound state and thus that the principal intermolecular interaction binding NH_3 at the interface involves a hydrogen bond with a free OH.

With this idea in mind, the ab initio results show that there is a significantly greater binding energy of ammonia to two hydrogen-bonded water molecules than there is to a single water molecule. This greater binding energy arises from the formation of a second hydrogen bond, with NH_3 as the donor and the second H_2O molecule as the acceptor. The calculated binding enthalpy of NH_3 to a water dimer is slightly less than the ΔH_{ads}° obtained experimentally. A simple model of the surface interactions, which assumes them to be essentially the same as those in $NH_3-(H_2O)_2$, yields predicted values of ΔS_{ads}° and ΔG_{ads}° in reasonable agreement with the experimental values as well. We conclude that most of the important features of the surface-bound state are captured in a model in which the ammonia molecule interacts simultaneously with two mutually hydrogen-bonded water molecules. The primary interaction is via hydrogen bonding to a free OH at the surface. The differences between the calculated and measured thermochemical parameters may reflect deficiencies in how the adsorption entropy is estimated or may indicate that a third water molecule is weakly involved.

The evaporation rate constants derived from the time dependence of the surface coverage suggest that the free energy of activation for evaporation of NH_3 from its surface-bound state is simply the desorption free energy; there is no free energy barrier other than the endothermicity of the process. A further implication is that any free energy barrier separating the solution and surface states is much smaller than ΔG_{ads}° from the gas phase and so does not affect the evaporation kinetics. This implies facile transfer of the solvated ammonia to the interface prior to its evaporation.

Strictly speaking, the kinetics presented here represent an approximation to the "true" evaporation kinetics, since the analysis relies upon an assumption of quasi-equilibrium between the solution and surface states. If this assumption held rigorously, we would observe a decrease in the solution concentration commensurate with the decrease in the surface coverage. A better picture might assume quasi-equilibrium between the surface state and the solution lying within a "diffusion length" of the interface; this solution would be in a slower equilibrium with the bulk, through diffusion. Such a rapid exchange of molecules within the first several layers of the surface is consistent with the highly dynamic nature of the water−air interface. Since the more concentrated solutions undergo smaller decreases in surface coverage over the time of the experiment, there is more opportunity for the bulk solution and near-surface

solution to remain in quasi-equilibrium for these solutions. Therefore, the kinetics derived from the more concentrated solutions are a closer approximation to the "true" kinetics, suggesting even closer agreement between the activation free energy for evaporation and the free energy of desorption.

The picture of the ammonia vapor−water surface interaction that emerges is consistent with the "critical cluster" model of Davidovits et al.[4] In that model transport of a trace species, X, between the gas phase and solution phase is mediated by the formation of X−water complexes at the air−water interface. True solvation occurs when clusters of some critical size are formed; these can transfer between the surface and solution phases without any barrier. This model suggests that a critical cluster size is one which captures most (or all) of the solvation free energy of X, since there would then be no barrier to transport into the bulk.

The present results suggest that ammonia in its surface-bound state is associated with two (or possibly three) water molecules. The principal intermolecular interactions at the surface are hydrogen bonds; ammonia acts as both a donor and an acceptor of these bonds at the interface. The free energy cost of transfer from the surface-bound state to the fully solvated state is primarily due to the decrease in entropy associated with the transfer. There may be a free energy barrier to the transfer in excess of the endothermicity, but if it exists it is much smaller than 20 kJ mol^{-1}.

Finally, the findings given here can be applied to the partitioning of ammonia between droplets and the gas phase in the troposphere. Assuming as a first approximation that the values of Γ^{sat} and b are independent of temperature, at 270 K and a gas-phase ammonia concentration of 1 ppb, the solution concentration is 2.6×10^{-7} molal and the surface excess is calculated to be 2.2×10^{7} molecules cm^{-2}. We may estimate that a water droplet of diameter 200 nm will contain approximately one NH_3 molecule and its surface will contain approximately 0.03 molecules. At a diameter of 50 nm (ignoring effects due to curvature), the surface concentration is predicted to be almost 20% of the bulk concentration. Under these circumstances, chemical reactions involving NH_3 will take place at the interface, as well as in the bulk.

Acknowledgment is made to the donors of the Petroleum Research Fund, administered by the ACS, and to NSERC for support of this research. Mr. D. Anderson measured the surface tensions used here. Many thanks to Drs. P. Davidovits, B. J. Finlayson-Pitts, M. C. Goh, J. A. Guest, D. R. Hanson, D. Ray, J. T. Roberts, and D. R. Worsnop who have provided many hours of entertaining and stimulating discussion on the subject of gas−liquid interactions.

References and Notes

(1) Seinfeld, J. H. *Atmospheric Chemistry and Physics of Air Pollution*; Wiley-Interscience: New York, 1986.

(2) Finlayson-Pitts, B. J.; Pitts, J. N., Jr. *Atmospheric Chemistry*; Wiley: New York, 1986.

(3) Donaldson, D. J.; Guest, J. A.; Goh, M. C. *J. Phys. Chem.* **1995**, *99*, 9313.

(4) Davidovits, P.; Hu, J. H.; Worsnop, D. R.; Zahniser, M. S.; Kolb, C. E. *Faraday Discuss.* **1995**, *100*, 65 and references therein.

(5) Karpovich, D. S.; Ray, D. *J. Phys. Chem. B* **1998**, *102*, 649.

(6) Micheli, L. I. A. *Philos. Mag.* **1927**, 895.

(7) Rice, O. K. *J. Phys. Chem.* **1928** *32*, 583−592.

(8) Cutting, C. L.; Jones, D. C. *J. Chem. Soc.* **1955**, 4067. Jones, D. C.; Ottewill, R. H. *Ibid.* **1955**, 4076.

(9) Hartkopf, A.; Karger, B. L. *Acc. Chem. Res.* **1973** *6*, 209 and references therein.

(10) Strathdee, G. G.; Given, R. M. *J. Phys. Chem.* **1976** *80*, 1714 and references therein.

(11) Jho, C.; Nealon, D.; Shogbola, S.; King, A. D., Jr. *J. Colloid Interface Sci.* **1978**, *65*, 141 and references therein.

(12) Baumer, D.; Mang, H.; Findenegg, G. H., *Ber. Bunsen-Ges. Phys. Chem.* **1978**, *82*, 878.

(13) Turkevich, L. A.; Mann, J. A. *Langmuir* **1990**, *6*, 445−457.

(14) Hoff, J. T.; Mackay, D.; Gillham, R.; Shiu, W. Y. *Environ. Sci. Technol.* **1993**, *27*, 2174 and references therein.

(15) Jayne, J. T.; Davidovits, P.; Worsnop, D. R.; Zahniser, M. S.; Kolb, C. E. *J. Phys. Chem.* **1990**, *94*, 604.

(16) Defay, R.; Prigogine, I.; Bellemans, A.; Everett, D.H. *Surface Tension and Adsorption*; Longmans, London, 1966.

(17) Kemball, C.; Rideal, E. K. *Proc. R. Soc. (London)* **1946**, *A187*, 53.

(18) Adamson, A. W. *Physical Chemistry of Surfaces*, 5th ed.; Wiley-Interscience: New York, 1990.

(19) Shoemaker, D. P.; Garland, C. W.; Nibler, J. W. *Experiments in Physical Chemistry*, 5th ed.; McGraw-Hill: New York, 1989.

(20) Bates, R. G.; Pinching, G. D. *J. Res. Natl. Bur. Stand.* **1949**, *42*, 419.

(21) Clegg, S. L.; Brimblecombe, P. *J. Phys. Chem.* **1989**, *93*, 7237.

(22) *CRC Handbook of Chemistry and Physics* 71st ed.; Lide, D. R., Ed.; CRC Press: Boca Raton, FL 1990.

(23) Masella, M.; Flament, J. P. *J. Chem. Phys.* **1998**, *108*, 7141.

(24) Frisch, M. J.; Trucks, G. W.; Schlegel, H. B.; Gill, P. M. W.; Johnson, B. G.; Robb, M. A.; Cheeseman, J. R.; Keith, T.; Petersson, G. A.; Montgomery, J. A.; Raghavachari, K.; Al-Laham, M. A.; Zakrzewski, V. G.; Ortiz, J. V.; Foresman, J. B.; Cioslowski, J.; Stefanov, B. B.; Nanayakkara, A.; Challacombe, M.; Peng, C. Y.; Ayala, P. Y.; Chen, W.; Wong, M. W.; Andres, J. L.; Replogle, E. S.; Gomperts, R.; Martin, R. L.; Fox, D. J.; Binkley, J. S.; Defrees, D. J.; Baker, J.; Stewart, J. P.; Head-Gordon, M.; Gonzalez, C.; Pople, J. A. *Gaussian 94, Revision D.3*; Gaussian, Inc.: Pittsburgh, PA, 1995.

(25) Pople, J. A.; Scott, A. P.; Wong, M. W.; Radom, L. *Isr. J. Chem.* **1993**, *33*, 345.

(26) Stone, A. J. *The Theory of Intermolecular Forces*; Clarendon Press: Oxford, 1996.

(27) Boys, S. F.; Bernardi, F. *Mol. Phys.* **1970** *17*, 553.

(28) Dyke, T. R.; Herbine, P. *J. Chem. Phys.* **1985**, *83*, 3768.

(29) Herbine, P.; Hu, T. A.; Johnson, G.; Dyke, T. R. *J. Chem. Phys.* **1990**, *93*, 5485.

(30) Stockman, P. A.; Bumgarner, R. E.; Suzuki, S.; Blake, G. A. *J. Chem. Phys.* **1992**, *96*, 2496.

(31) Fraser, G. T.; Suenram, R. D. *J. Chem. Phys.* **1992**, *96*, 7287 and references therein.

(32) Astrand, P.-O.; Karlstrom, G.; Engdahl, A.; Nelander, B. *J. Chem. Phys.* **1995**, *102*, 3534 and references therein.

(33) Sosa, C. P.; Carpenter, J. E.; Novoa, J. J. *Chemical Applications of Density-Functional Theory*; American Chemical Society: Washington, DC, 1996.

(34) Latajka, Z.; Scheiner, S. *J. Phys. Chem.* **1990**, *94*, 217.

(35) Schenter, G. K. *J. Chem. Phys.* **1998**, *108*, 6222 and references therein.

(36) Du, Q.; Superfine, R.; Freysz, E.; Shen, Y. R. *Phys. Rev. Lett.* **1993,** *70*, 2313.

(37) Herzberg, G. *Molecular Spectra and Molecular Structure III. Electronic Spectra and Electronic Structure of Polyatomic Molecules*; van Nostrand Reinhold: New York, 1966.